





Evaluation of in vitro SARS-CoV-2 inactivation by a new quaternary ammonium compound: Bromiphen bromide

Sergio Strizzi¹  | G. Cappelletti¹ | M. Biasin¹ | Angelica Artasensi²  |
Laura Fumagalli²  | Antonella Casiraghi² 

¹Department of Biomedical and Clinical Sciences, University of Milan, Milan, Italy

²Department of Pharmaceutical Sciences, University of Milan, Milan, Italy

Correspondence

Laura Fumagalli, Department of Pharmaceutical Sciences, University of Milan, Via Mangiagalli 25, 20133, Milan, Italy.
Email: laura.fumagalli@unimi.it

Funding information

Università degli Studi di Milano; University of Milan, Seed for Innovation Patent—SEED4IP—WANTED Project

Abstract

The pneumonia (COVID-19) outbreak caused by the novel coronavirus named severe acute respiratory syndrome coronavirus 2 (SARS-CoV-2), which unpredictably exploded in late December of 2019 has stressed the importance of being able to control potential pathogens with the aim of limiting their spread. Although vaccines are well known as a powerful tool for ensuring public health and controlling the pandemic, disinfection and hygiene habits remain crucial to prevent infection from spreading and maintain the barrier, especially when the micro-organism can persist and survive on textiles, surfaces, and medical devices. During the coronavirus disease pandemic, around half of the disinfectants authorized by the US Environmental Protection Agency contained quaternary ammonium compounds (QACs); their effectiveness had not been proven. Herein, the in vitro SARS-CoV-2 inactivation by *p*-bromodomiphen bromide, namely bromiphen (BRO), a new, potent, and fast-acting QAC is reported. This study demonstrates that BRO, with a dose as low as 0.02%, can completely inhibit SARS-CoV-2 replication in just 30 s. Its virucidal activity was 10- and 100-fold more robust compared to other commercially available QACs, namely domiphen bromide and benzalkonium chloride. The critical micellar concentration and the molecular lipophilicity potential surface area support the relevance of the lipophilic nature of these molecules for their activity.

KEYWORDS

COVID-19, critical micellar concentration, disinfectants, sanitizer, virucidal activity

1 | INTRODUCTION

In late December 2019, the pneumonia outbreak, known as COVID-19 caused by the novel coronavirus severe acute respiratory syndrome coronavirus 2 (SARS-CoV-2), emerged, leading to an

unexpected and alarming impact on health, society, and the economy. Although the development of many safe and effective SARS-CoV-2 vaccines made it foresee the eradication of the pandemic, the patency of continuous breakthrough infections and the high infectivity rate advocates for the enactment of disinfection and

Sergio Strizzi and G. Cappelletti contributed equally to this work.

This is an open access article under the terms of the Creative Commons Attribution License, which permits use, distribution and reproduction in any medium, provided the original work is properly cited.

© 2023 The Authors. *Archiv der Pharmazie* published by Wiley-VCH GmbH on behalf of Deutsche Pharmazeutische Gesellschaft.

prevention strategies to limit the spread of SARS-CoV-2 and hopefully other unpredictable viral infections that could arise in the future.

Indeed, although SARS-CoV-2 transmission mainly occurs through direct-route by aerosol respiratory droplets generated through coughing and sneezing by infected individuals, in a significant number of COVID-19 cases, epidemiological investigations could not find evidence of direct close contact with other confirmed patients; therefore, at least some of these cases may be caused by indirect transmission. The latter includes the contamination of hands or inanimate/inert surfaces (fomites) on which the virus can survive, followed by touching the mouth, nose, or eyes. Indeed, some viruses show the ability to transfer between and persist on different surfaces (from hours to days), including the human skin for that reason. Disinfection and hygiene habits remain crucial to avoid infection dissemination and to maintain the barrier. As a matter of fact, practical experience in different settings has widely demonstrated that the right choice of disinfectant agent,^[1] stringent disinfection, and control measures may be highly effective in limiting person-to-person transmission.

As an enveloped virus SARS-CoV-2 is particularly sensitive to detergents and disinfectants, that is why World Health Organization recommends cleaning surfaces and hands with these classes of compounds. However, SARS-CoV-2 is a relatively novel virus and a biosafety level-3 (BSL-3) agent, hence experimental data assessing the virucidal effect of these compounds on this specific pathogen are still limited and need to be implemented. In fact, our current knowledge is mainly based on previous coronavirus studies reporting disinfectants, such as ethanol (>62% concentration), isopropanol, sodium hypochlorite, and quaternary ammonium compounds (QACs) combined with alcohol are able to contain coronavirus infections. In particular, QACs are organic compounds featuring a positively charged nitrogen atom, making them effective antimicrobial agents. These compounds exhibit a wide range of structural diversity and can be tailored for specific applications. QACs are commonly used as disinfectants, preservatives, and surfactants due to their ability to disrupt cell membranes with well-known broad-spectrum antimicrobial activities, hence representing a repurposing opportunity as disinfectants against SARS-CoV-2. The hydrophilic head, a cationic ammonium group, is what gives them their distinctive properties. The ammonium group has four organic substituents, including alkyl or heterocyclic groups, which create the lipophilic tail. An anion, such as a halide or sulfate, balances the charge. Thanks to these specific

features they eradicate surface bacteria and common viruses such as influenza by solvating and rupturing their lipid membranes or envelopes. Actually, QACs target microbial cell membranes through electrostatic interactions between the positively charged headgroup and negatively charged cytoplasmic membrane, then adsorption occurs, and insertion of their side chains into the intramembrane region takes place.^[2,3] Thus the lipid layer of enveloped viruses, such as SARS-CoV-2, makes them sensitive to the hydrophobic activity of QACs.^[4-6] This success was confirmed, during the coronavirus pandemic disease when around half of the disinfectants authorized by the US Environmental Protection Agency contained QACs as active components against a wide range of microbes.^[7,8] Indeed, their efficacy on SARS-CoV-2 inactivation has been recently demonstrated by some authors in different experimental conditions.^[9,10] In particular, Ijaz et al.^[9] demonstrated that 0.1% benzalkonium chloride (BAK) inactivates SARS-CoV-2 within 2 min in carrier test. Likewise, Xiling et al.^[10] verified that the QAC disinfectants, di-N-decyltrimethylammonium bromide and di-N-decyltrimethylammonium chloride, exhibit high efficiency with low dose effectiveness and short reaction times, claiming a more significant role of QACs in the global fight against COVID-19.

On the basis of these premises, finding a new virucidal compound and implementing experimental data concerning SARS-CoV-2 is persistently necessary. Notably, quite recently a new QAC, namely bromiphen bromide (BRO), has been characterized by means of liquid chromatography electrospray ionization tandem mass spectrometry (LC-ESI-MS/MS) and high-performance liquid chromatography analyses.^[11,12] These studies revealed that BRO is stable under acidic and oxidizing conditions and also under thermal stress. BRO antimicrobial activity, mainly against Gram-positive strains, has been verified as well; but no one has so far proved that this new compound may display also antiviral activity and the minimum dose necessary to effectively inhibit SARS-CoV-2. Thus, in this study, we tested the virucidal effect of BRO on SARS-CoV-2 infection/replication in comparison with two other commercially available QACs, domiphen bromide (DOM) and BAK (Figure 1). DOM was chosen because it is already used in commercially available pharmaceutical preparation and is very similar to BRO from a structural point of view. In fact, they differ for a bromide atom instead of a hydrogen one at the *para* position of the aromatic ring. BAK was selected as a benchmark because, in addition to belonging to the same chemical class as BRO, it is present in several medical devices already in the market.

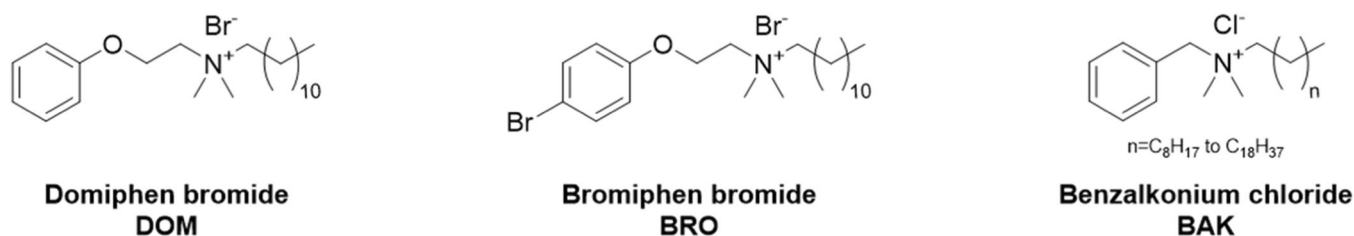


FIGURE 1 Structures of Domiphen bromide (DOM), Bromiphen bromide (BRO), and Benzalkonium chloride (BAK).

2 | RESULTS AND DISCUSSION

2.1 | Pharmacology/biology

2.1.1 | BRO, DOM, and BAK cytotoxicity and neutralization assessment

3-(4,5-Dimethylthiazol-2-yl)-2,5-diphenyltetrazolium bromide (MTT) analyses showed that all three QACs exert a cytotoxic effect at the highest concentrations used in the following experiments: 0.2%–0.002% (Figure 2a–c, MTT). Such cytotoxic effect abruptly disappeared at 0.0002% for all three tested compounds, while at 0.002% BRO and DOM showed a less pronounced cytotoxic effect compared to BAK. Considering their impact on cell viability, to effectively test their virucidal activity in an in vitro infection assay, all compounds were inactivated by incubation with a neutralizer solution. This was done before transferring the (virus + QAC) mix into the cell culture to neutralize any potential residual of their cytotoxic effect. Moreover, as shown in Figure 2d, the cytotoxicity of the neutralizer was also assessed by confirming that it did not affect cell viability from 1:10 dilution onwards.

Then, to evaluate the neutralizer capability of completely removing the cytotoxic effect, the highest BRO concentration (0.2%) was used according to the setting reported in Table 3 (see below in Section 4). The results obtained are reported in Figure 3. In Test 1, the inhibition of viral replication was due to the cytotoxic effect exerted by BRO on VeroE6 cells, as shown by cytopathic effect (CPE) monitoring (Figure 3b). Notably, in Test 2, the neutralizer solution effectively inhibited BRO cytotoxicity when used in a 9:10 ratio (neutralizer:QAC) (Figure 3a). Moreover, neither the neutralizer (Test 3) nor the (disinfectant + neutralizer) mix (Test 4) had adverse effects on cell viability, indeed the virus was able to replicate. Neutralization analyses performed on DOM and BAK mirrored the results obtained with BRO (data not shown). Hence,

the neutralizer was selected as a QAC inactivator in all the SARS-CoV-2 infection tests performed in the study.

2.1.2 | Inhibition of SARS-CoV-2 replication in VeroE6 cells

To determine the minimum QAC virucidal concentration an in vitro infection assay exposing SARS-CoV-2 for 30 s to serial QAC dilutions (0.02%–0.002%–0.0002%–0.00002%–0.000002%–0.0000002%) was performed. After the exposure period, QACs were neutralized and then the diluted samples containing 25 TCID₅₀/mL and QACs were seeded in cells. Viral replication was assessed at different times, namely at 18 (T1), 48 (T2), and 72 (T3) hours postinfection (hpi), respectively. Results show that BRO is able to inactivate SARS-CoV-2 just following 30 s of incubation, as shown in Figure 4a. In particular, a dose of 0.02% was sufficient to completely inhibit viral replication at T1 and to maintain such an effect over time. Conversely, the 0.002% concentration controlled viral replication at T1 and T2 but it was no longer efficacious at T3. Notably, the virucidal effect displayed by BRO showed a dose–response trend at T2 (Figure 4b). T1 and T3 were unfunctional timepoints to appreciate a dose–response trend as shown in Figure 4a. Indeed, at T1 there were no viral particles even in the untreated condition, whereas, at T3 the viral replication reached a plateau.

The same tests were performed by incubating SARS-CoV-2 with DOM (Figure 4c) or BAK (Figure 4d). Results mirrored those obtained by BRO treatment. However, BRO virucidal activity was 10- and 100-fold more efficient compared to DOM and BAK, respectively. Indeed, a concentration of 0.002% of DOM was unable to inhibit viral replication at T2 (Figure 4c). Moreover, BAK was even less efficacious compared to BRO and DOM as its virucidal activity was displayed and maintained over time only with a 0.2% concentration (Figure 4d).

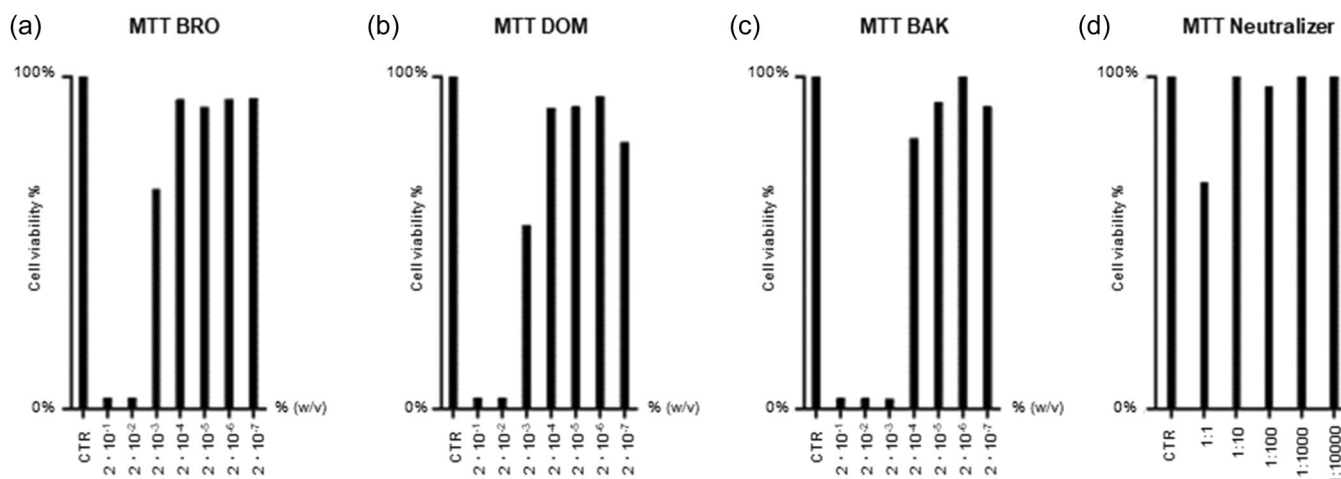


FIGURE 2 Cell viability assessment by MTT assay. Percentage of cell viability after VeroE6 culture with different doses of (a) BRO, (b) DOM, and (c) BAK: 0.2%, 0.02%–0.002%–0.0002%–0.00002%–0.000002%–0.0000002% at 72 h assessed using an MTT assay. (d) Cell viability assessment following neutralizer exposure at different dilutions: 1:1, 1:10, 1:100, 1:1000, 1:10,000. BAK, benzalkonium chloride; BRO, bromphen bromide; DOM, domiphen bromide; MTT, 3-(4,5-dimethylthiazol-2-yl)-2,5-diphenyltetrazolium bromide.

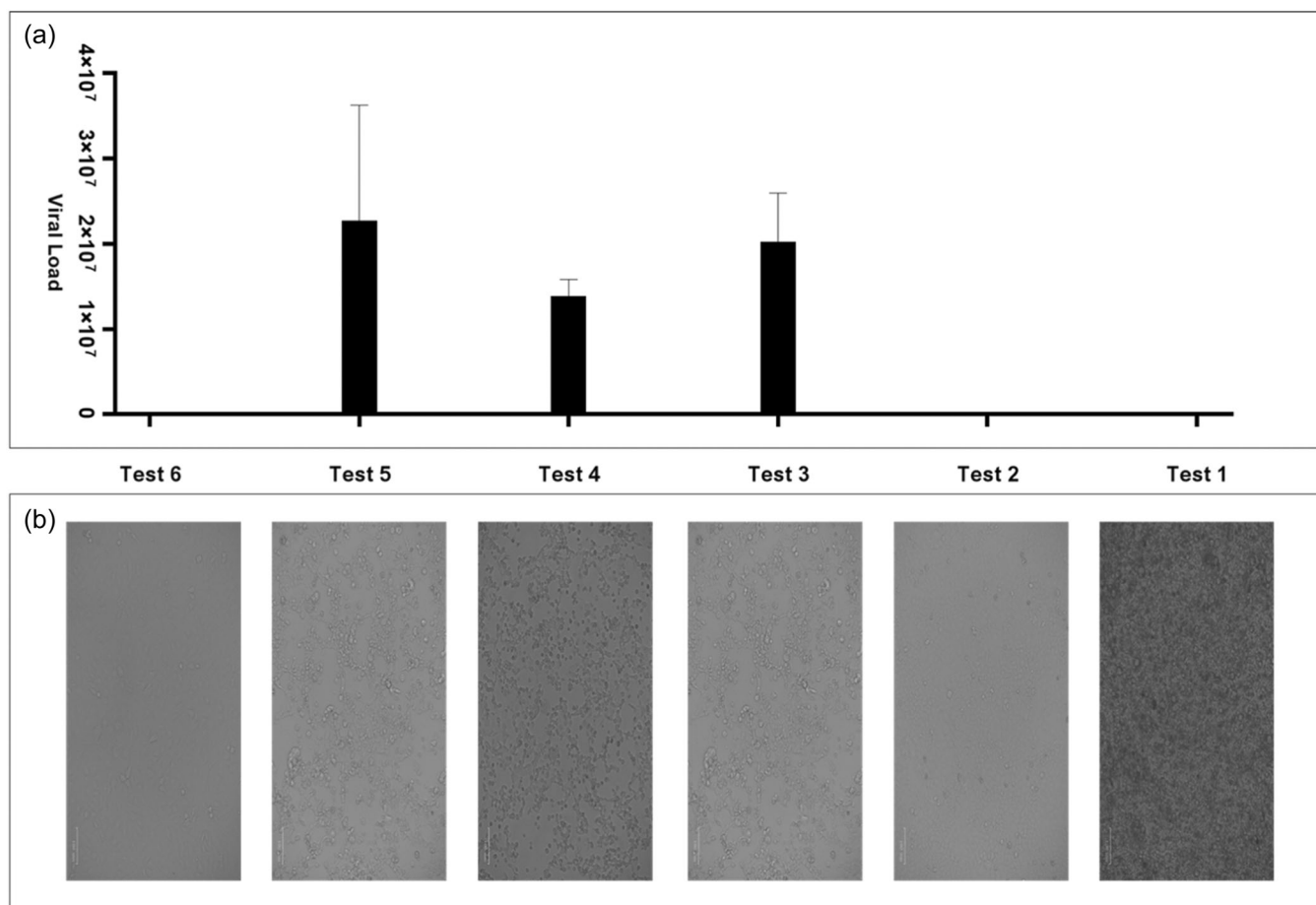


FIGURE 3 Evaluation of neutralizer capability in inhibiting cytotoxic effect of BRO. The neutralizer capability was evaluated by means of viral load calculation after (a) SARS-CoV-2 infection assay and (b) CPE monitoring. The picture above shows the results of the following tests: Test 1: disinfectant + virus, Test 2: (disinfectant + virus) + neutralizer, Test 3: neutralizer + virus, Test 4: (disinfectant + neutralizer) + virus, Test 5: virus, Test 6: cellular controls. BRO, bromiphen bromide; CPE, cytopathic effect; SARS-CoV-2, severe acute respiratory syndrome coronavirus 2.

2.1.3 | Determination of critical micellar concentration and lipophilic analysis

BRO, as well as other QACs, is an amphiphilic molecule, commonly known as a surfactant, composed of a hydrophobic and a hydrophilic portion. Based on these chemical-physical characteristics, QACs' activity has often been associated with micelle formation. Micelles are supramolecular aggregates; in a physiological environment, hydrophilic heads are exposed outside, in touch with the aqueous environment, while the hydrophobic tails are packed together to form the core. The physical state of surfactants as unimers or micelles has a significant impact on their behavior. The discussion about the role of micelle formation and surfactant ability to disrupt biological membranes is still open, even if the nondependence of the activity with respect to the critical micelle concentration (CMC) value was recently highlighted and virus inactivation below and above the determined CMC was confirmed.^[13,14]

For these reasons, it is worth knowing the self-assembling properties of the tested substances. Thus, the CMC of BRO was determined by measuring the electrical conductivity of aqueous dispersions at

increasing concentrations. To understand completely the mechanism and how it influences the virucidal activity highlighted and to support the determination of BRO CMC (never calculated before) the measurement was also performed on cetylpyridinium chloride (CPC), DOM, and BAK. In general, the CMC of surfactants mainly depends on their hydrophobicity; this means that CMC values decrease rapidly, increasing the hydrophobic moiety of a molecule.

The obtained CMC values (Table 1) using conductometric measurements^[23] were in good agreement with previously published results. The CMC value of BRO can therefore be considered reliable.

Conductivity measured for each dispersion at increasing percentages (Supporting Information: Table S1) and graphical representation according to Williams' method and Phillips' methods (Supporting Information: Figures S1-S4) are reported in Supporting Information.

From the obtained results, BRO shows the lowest CMC compared to DOM and BAK, highlighting a more pronounced hydrophobic nature of the new compound. Moreover, the CMC trend parallels the virucidal activity one. In fact, the lowest is the CMC the highest is the activity of the compound. It was also evidenced that BRO is active at a concentration (0.02%) lower than

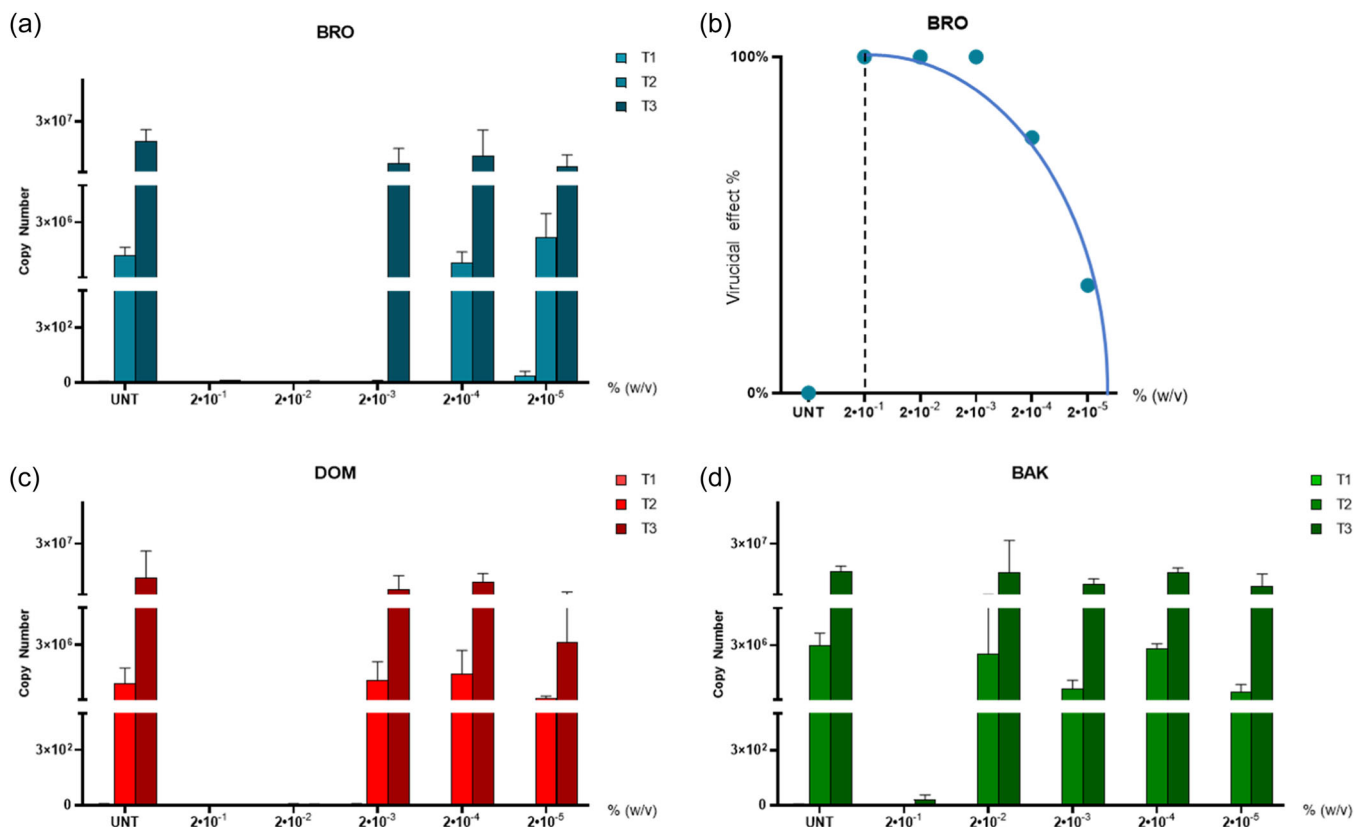


FIGURE 4 SARS-CoV-2 incubation with QACs inhibits VeroE6 cell infection. VeroE6 cells were incubated with different concentrations of (a) BRO, (c) DOM, and (d) BAK. Virus mixtures and viral replication were assessed at different time points T1 (18 hpi), T2 (48 hpi), and T3 (72 hpi). Dose–response trend of BRO at T2 (b). To avoid the QAC cytopathic effect, all QAC-virus mixtures were exposed to the neutralizer in a 9:10 ratio before inoculum on VeroE6 cells. BRO, DOM, and BAK virucidal effects occur at 0.002%, 0.02%, and 0.2% concentration, respectively. Results correspond to the absolute viral copy number of the SARS-CoV-2 N1 gene from cell supernatants that were quantified through a single-step, real-time, RT-qPCR by referring to a standard curve from RT-qPCR C_t values (IDT). Results are presented as mean ± SEM from at least *n* = 3 independent experiments, each performed in triplicate. BAK, benzalkonium chloride; BRO, bromiphen bromide; DOM, domiphen bromide; hpi, hours postinfection; QAC, quaternary ammonium compound; RT-qPCR, quantitative reverse transcription polymerase chain reaction; SARS-CoV-2, severe acute respiratory syndrome coronavirus 2; UNT, untreated control.

TABLE 1 Determined CMC according to conductometric analysis.

	Williams method (g/100 mL) ^[15]	Phillips method (g/100 mL) ^[16]	CMC reported literature (%)
CPC	0.03425	0.03442	0.03060–0.03400 ^[17,18]
DOM	0.06806 ± 0.000145	0.06748	0.06210–0.07452 ^[19,20]
BAK	0.14728	0.14356	0.17 ^[21,22]
BRO	0.03041 ± 0.00025	0.02898	—

Note: Details on data and graphical representation are reported in Supporting Information Materials.

Abbreviations: BAK, benzalkonium chloride; BRO, bromiphen bromide; CMC, critical micelle concentration; CPC, cetylpyridinium chloride; DOM, domiphen bromide.

the CMC, suggesting that BRO activity in the tested solution is not due to organization in micelle aggregates. As already reported by Farcet et al.^[14] for other detergents, the efficacy of BRO against virus can be detected below the CMC confirming that virus inactivation is

not strictly related to micelle formation. Moreover, the difference in determined CMC for BRO and DOM that share structure similarities can be justified by diverse lipophilicity, which, in turn, can explain the better ability of BRO to disrupt biological membranes, thus resulting in a lower active concentration. Figure 5 reports the molecular lipophilicity potential (MLP) surface of DOM (Figure 5a) and BRO (Figure 5b). In MLP maps, color codes were used as follows: hydrophilic surfaces are defined by blue regions; violet/purple regions show the most lipophilic surfaces. Last, intermediate lipophilic surfaces are colored yellow. The violet/purple zones that represent the lipophilic surfaces are more intense in BRO (Figure 5b) than in DOM (Figure 5a). On the other hand, in the MLP diagram referred to DOM the yellow intermediate lipophilic area originating from the unsubstituted aromatic region is more dominant. Therefore, as shown by MLP maps, BRO is expected to be more lipophilic than DOM.

Furthermore, the analysis of the lipophilic character of both DOM and BRO through WLOGP, MLOGP, iLOGP, XLOGP3, and SILICOS-IT predictive models was performed via SwissADME

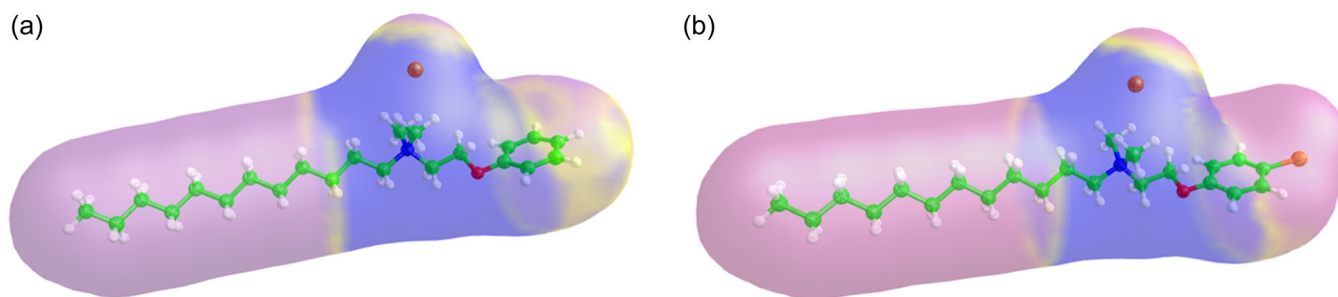


FIGURE 5 MLP diagrams of (a) DOM and (b) BRO. BRO, bromiphen bromide; DOM, domiphen bromide; MLP, molecular lipophilicity potential.

TABLE 2 Estimations of physicochemical properties and $\log P_{ow}$ values for DOM and BRO.

Physicochemical properties			Lipophilicity $\log P$		
	DOM	BRO		DOM	BRO
Molecular weight	414.46	493.36	iLOGP	-1.98	-1.95
No. of heavy atoms	25	26	XLOGP3	8.50	9.19
No. of aromatic heavy atoms	6	6	WLOGP	3.07	3.83
Fraction Csp3	0.73	0.73	MLOGP	1.46	2.05
No. of rotatable bonds	15	15	Silicos-IT $\log P$	3.68	4.39
No. of H-bond acceptors	1	1	Consensus $\log P$	2.95	3.50
No. of H-bond donors	0	0			
Molar refractivity	116.34	124.04			
TPSA	9.23	9.23			

Abbreviations: BRO, bromiphen bromide; DOM, domiphen bromide; TPSA, topological polar surface area.

software.^[24] Table 2 reports estimations and consensus $\log P_{ow}$ values for DOM and BRO. For BRO, the consensus $\log P_{ow}$ value was calculated as 3.50. Since bromide substitution is known to increase lipophilicity, also considering the more classical Hammett constant, the result obtained is quite reasonable. At this point, SwissADME and VEGA ZZ^[25] analysis results support each other.

3 | CONCLUSION

Through this study we demonstrate that BRO can completely inhibit SARS-CoV-2 replication in just 30 s and with a dose as low as 0.02%, supporting the recommendation of BRO as a candidate commodity that could be used to kill SARS-CoV-2 and potentially other enveloped viruses. Importantly, BRO virucidal activity was 10- and 100-fold more robust compared to DOM and BAK, respectively. Moreover, the use of

BRO would allow for a reduction in the dose of QAC disinfectants to be used, which would be extremely advantageous to minimize the environmental load of QACs. Indeed, it cannot be overlooked that elevated QAC exposure has been supposed to favor the spread of antibiotic resistance and cause other environmental issues.^[3,26,27]

The mechanism of action of BRO is believed to occur as a result of perturbation of the virally modified, host-cell-derived, phospholipid bilayer glycoprotein envelope, and the associated spike glycoproteins that bind with the angiotensin-converting enzyme receptor required for infection of host cells likewise reported for other formulated microbicidal compounds and detergents.^[28,29] As far as its behavior is concerned, BRO seems to be active even under its CMC thus maintaining activity also as unimer. CMC and MLP support that the virus inactivation is independent of the CMC but rather strictly related to the lipophilic nature of the molecules. It might be worth investigating further whether it is possible to define a limit on the lipophilic characteristic of a potentially active molecule.

4 | EXPERIMENTAL

4.1 | Experimental design

The primary endpoint of the study was to assess the virucidal effect of the BRO compound on SARS-CoV-2 and to establish its minimal effective dose. The secondary endpoints were: (i) to test the CPE of these disinfectants, (ii) to compare the BRO effect to two other QACs already commercially available, namely DOM and BAK, and (iii) to identify BRO critical micellar concentrations.

To assess all these aims a specific viral titer was exposed to scalar disinfectant concentrations and its virucidal effect was tested in an in vitro infection assay as later described.

4.2 | Cell lines, virus, and reagents

VeroE6 (CRL-1586™, African green monkey kidney epithelial cells) cells were purchased from the American Type Culture Collection

(ATCC®). Cells were grown in Dulbecco's modified Eagle medium (DMEM) high glucose (ECB20722L; Euroclone), supplemented with 10% fetal bovine serum (FBS), and 1% L-glutamine and PenStrep. Cells were grown at 37°C in 5% CO₂ and at 98% humidity. Cells were routinely checked for mycoplasma contamination by polymerase chain reaction (PCR) test. Cells between passages 15 and 25 were used for the experiments.

SARS-CoV-2 virus human 2019-nCoV (strain 2019-nCoV/Italy-INMI1) was expanded in VeroE6 cells and infectious viral particle concentration was assessed by TCID₅₀ endpoint dilution assay as previously described.^[30] The TCID₅₀ for viral titers exposed to the disinfectants in each test was 2.5×10^5 TCID₅₀/mL.

All the experiments with the SARS-CoV-2 virus were performed in the BSL-3 facility; before sample analysis outside the BSL-3 area, the virus was disabled according to institutional safety guidelines.

The following reagents were used in the cell culture assays: BRO was synthesized by our laboratories according to the procedures already published^[11,12,31]; DOM and BAK were purchased from Merck KGaA and used as commercially distributed.

4.3 | MTT assay

The cytotoxic effect of BRO, DOM, and BAK was evaluated by means of MTT assay: VeroE6 cells were seeded in 96-well plates (2×10^4 per well) for 24 h and treated with different BRO, DOM, and BAK concentrations: 0.02%–0.002%–0.0002%–0.00002%–0.000002%–0.0000002%. The concentrations were decided by considering the active doses of BRO, DOM, and BAK as previously reported.^[12] After 72 h, cell viability was assessed by the MTT method.

Briefly, 30 µL of MTT (final concentration, 0.5 mg/mL) was added to each well under sterile conditions, and the 96-well plates were incubated for 4 h at 37°C. Supernatants were removed, and dimethyl sulfoxide (100 µL/well) was added. The plates were then agitated on a plate shaker for 5 min. The absorbance of each well was measured at 490 nm with a Bio-Rad automated EIA analyser (Bio-Rad Laboratories). The viability of untreated cells (control) was considered 100%, while the other conditions were expressed as percentages of control.

The MTT test was performed even on different neutralizer concentrations (1:1, 1:10, 1:100, 1:1000, 1:10,000).

4.4 | Neutralizer efficacy assessment

Since all the highest concentrations of the tested compounds proved to exert a cytotoxic effect on VeroE6 cell lines in an MTT assay, a composite that was able to stop the disinfectant's action (neutralizer) was employed. Neutralizing agents need to have an appropriate disabling effect on the chemical disinfectant and must not display detrimental or adverse effects on the virus and cell line used in the in vitro infection assay. To verify all these conditions, we conceived six

TABLE 3 Tests performed to assess the neutralizing agent efficacy.

Test 1	Disinfectant + virus
Test 2	(Disinfectant + virus) + neutralizer
Test 3	Neutralizer + virus
Test 4	(Disinfectant + neutralizer) + virus
Test 5	Virus
Test 6	Cellular controls

series of tests for each compound to depict the neutralization efficacy as shown in Table 3.

We performed this by incubating the highest QAC concentrations (0.2%) used in the subsequent experiments, with/without neutralizer (9:10 QAC concentration) in a test tube for 5 min and adding 2.5×10^5 TCID₅₀/mL of virus suspension and mixing well. The mixture was then used in an in vitro infection assay and viral replication was assessed by the culture-PCR (C-RT-PCR) method,^[32] as detailed in the following. In parallel, the CPE induced by SARS-CoV-2, QACs, and/or neutralizers was assessed. The neutralizer composition has been previously described in Wood et al.'s^[33] study.

4.5 | In vitro SARS-CoV-2 infection assay and virucidal effect evaluation

The 2.5×10^5 TCID₅₀/mL viral suspension was mixed with each of the three QACs at different concentrations and allowed to react for 30 s. Then, 0.1 mL of the reaction solution was added to a test tube containing 0.9 mL of the neutralizer solution (1:10) and mixed for 5 min, before undergoing two 10-fold series dilutions with DMEM (ECB7501L; Euroclone) as reported in Figure 6. The diluted samples containing 25 TCID₅₀/mL and 0.0002% QAC were seeded onto a 24-well cell culture plate (1.5×10^5 VeroE6 cells/well) with cells growing into monolayers and three wells for each concentration. After 1 h at 37°C and 5% CO₂ cells were rinsed two times with warm phosphate buffer saline, replenished with DMEM with 10% FBS medium, with 100 U/mL penicillin and 100 µg/mL streptomycin and observed daily for cytopathic effect (CPE). Viral replication was assessed by an integrated C-RT-PCR method at 18 (T1), 48 (T2), and 72 (T3) hpi in cell culture supernatants, as well as by analyzing SARS-CoV-2-induced CPE. RNA was extracted from VeroE6 cell culture supernatant by the Maxwell RSC Instrument with Maxwell RSC Viral Total Nucleic Acid Purification Kit (Promega). Real-time PCR was performed on a CFX96 (Bio-Rad) using the 2019-nCoV CDC qPCR Probe Assay emergency kit (IDT), which targets two regions (N1 and N2) of the nucleocapsid gene of SARS-CoV-2 (N2 data not shown). Reactions were performed according to the following thermal profile: initial denaturation (95°C, 10 min) followed by 45 cycles of 15 s at 95°C (denaturation) and 1 min at 60°C (annealing-extension). Viral copy quantification was assessed by creating a standard curve from the quantified 2019-nCoV_N positive Plasmid Control (IDT).

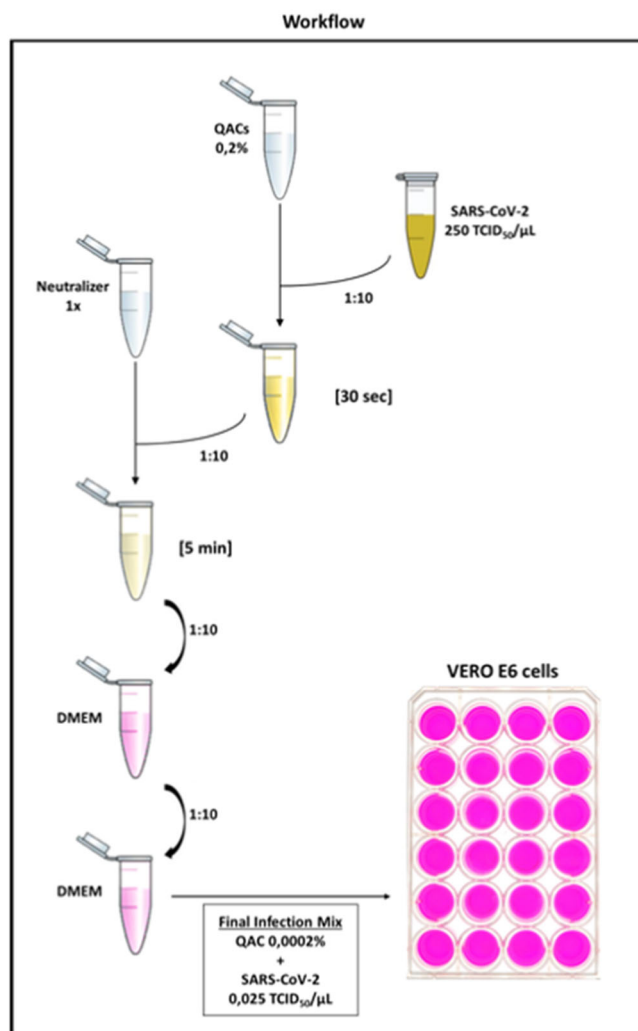


FIGURE 6 Experimental protocol adopted to test QACs (BRO, DOM, and BAK) antiviral activity, cytotoxicity, and neutralizer efficacy. Each compound was neutralized after being mixed with SARS-CoV-2. Two serial 1:10 dilutions in 10% FBS DMEM were carried out to further dilute the compound and thus reduce its cytotoxicity before performing the *in vitro* SARS-CoV-2 infection assay in VeroE6 cells. BAK, benzalkonium chloride; BRO, bromiphen bromide; DMEM, Dulbecco's modified Eagle medium; DOM, domiphen bromide; FBS, fetal bovine serum; QAC, quaternary ammonium compound; SARS-CoV-2, severe acute respiratory syndrome coronavirus 2.

Both positive and negative controls were performed for each test. The positive control used DMEM instead of QACs (untreated), and the negative control group used only DMEM. Each test was repeated three times.

4.6 | Statistical analyses

Overall, we performed three independent experiments according to the scheme reported in Figure 6. Statistical analyses were performed using GraphPad Prism 8. Results are expressed as mean \pm SEM of the

indicated *n* values. The two-tailed Student's *t*-test was used with a *p*-value threshold of 0.05.

4.7 | CMC and lipophilic analysis

4.7.1 | Preparation of aqueous dispersions

CPC, DOM, BAK, and BRO were dispersed in Milli-Q[®] water at a concentration equal to approximately four times the estimated CMC. Each surfactant was weighed and transferred into a 20 mL volumetric flask, to which water was added until the flask was approximately 95% filled; the flask was left for an hour at room temperature under magnetic stirring to allow the surfactant to form a homogenous dispersion; water was added until the flask was 100% full.

4.7.2 | Conductometric analysis

The specific conductivity ($\mu\text{S}/\text{cm}$) of surfactant solutions in water was measured at 20–23°C using a pH/conductivity meter (SevenCompact Duo S213; Mettler Toledo).

MilliQ water (20 mL) was placed in a 50-mL Falcon tube and its conductivity was measured. Aliquots of 1 mL of the initial dispersion were added to the water using a pipette (P1000 Gilson), and after each addition the tube was closed and shaken several times, following which the conductivity was measured. DOM and BRO experiment was performed in duplicate.

The determination of the CMC of ionic surfactants is based on the principle that the increase of an ionic surfactant concentration in water leads to a linear increase in conductivity until the CMC is reached. After this point, the conductivity will continue to increase linearly with the concentration, but with a lower slope.^[34]

The electrical conductivity measured after each addition was then plotted against the millimolar concentration of the surfactant. The two linear portions of the graph were identified, and linear regression analysis was used to obtain the equation of both. Finally, the surfactant concentration at the point of intersection, which corresponds to the CMC, was calculated (Williams method).^[15] To confirm this result, the second derivative of conductivity was also plotted, and the minimum of the corresponding Gaussian fit was found (Phillips method).^[15]

4.7.3 | MLP calculation

MLP surface areas of DOM (Figure 5a) and BRO (Figure 5b), with a probe radius of 0.7 and mesh size of 0.60, were generated and analyzed using Vega ZZ version 3.2.4.^[25]

ACKNOWLEDGMENTS

This research has received funding from the University of Milan, Seed for Innovation Patent—SEED4IP—WANTED Project.

CONFLICT OF INTEREST STATEMENT

Laura Fumagalli is one of the main inventors of the new patented compound bromiphen bromide.

ORCID

Sergio Strizzi  <http://orcid.org/0000-0003-3203-4523>

Angelica Artasensi  <http://orcid.org/0000-0002-9121-3217>

Laura Fumagalli  <http://orcid.org/0000-0003-1917-3000>

Antonella Casiraghi  <http://orcid.org/0000-0003-3683-8510>

REFERENCES

- [1] A. Artasensi, S. Mazzotta, L. Fumagalli, *Antibiotics* **2021**, *10*, 613. <https://doi.org/10.3390/antibiotics10060613>
- [2] M. C. Jennings, K. P. C. Minbiole, W. M. Wuest, *ACS Infect. Dis.* **2015**, *1*, 288. <https://doi.org/10.1021/acsinfecdis.5b00047>
- [3] P. I. Hora, S. G. Pati, P. J. McNamara, W. A. Arnold, *Environ. Sci. Technol. Lett.* **2020**, *7*, 622. <https://doi.org/10.1021/acs.estlett.0c00437>
- [4] C. P. Gerba, *Appl. Environ. Microbiol.* **2015**, *81*, 464. <https://doi.org/10.1128/AEM.02633-14>
- [5] C. L. Schrank, K. P. C. Minbiole, W. M. Wuest, *ACS Infect. Dis.* **2020**, *6*, 1553. <https://doi.org/10.1021/acsinfecdis.0c00265>
- [6] S. Mahmoudi, M. M. Dehkordi, M. H. Asgarshamsi, *Biophys. Chem.* **2022**, *288*, 106824. <https://doi.org/10.1016/j.bpc.2022.106824>
- [7] US EPA. List N Tool: COVID-19 Disinfectants. **2023**. <https://cfpub.epa.gov/wizards/disinfectants/> (accessed: July 2023).
- [8] US EPA. EPA Approves 13 Products from List N as Effective Against SARS-CoV-2. **2023**. <https://www.epa.gov/newsreleases/epa-approves-13-products-list-n-effective-against-sars-cov-2> (accessed: July 2023).
- [9] M. K. Ijaz, K. Whitehead, V. Srinivasan, J. McKinney, J. R. Rubino, M. Ripley, C. Jones, R. W. Nims, B. Charlesworth, *Am. J. Infect. Control* **2020**, *48*, 972. <https://doi.org/10.1016/j.ajic.2020.05.015>
- [10] G. Xiling, C. Yin, W. Ling, W. Xiaosong, F. Jingjing, L. Fang, Z. Xiaoyan, G. Yiyue, C. Ying, C. Lunbiao, Z. Liubo, S. Hong, X. Yan, *Sci. Rep.* **2021**, *11*, 2418. <https://doi.org/10.1038/s41598-021-82148-w>
- [11] L. Fumagalli, A. Moretto, E. Gilardon, C. Picozzi, G. Vistoli, M. Carini, *Data Brief* **2018**, *20*, 1363. <https://doi.org/10.1016/j.dib.2018.08.152>
- [12] L. Fumagalli, L. G. Regazzoni, V. Straniero, E. Valoti, G. Aldini, G. Vistoli, M. Carini, C. Picozzi, *J. Pharm. Biomed. Anal.* **2018**, *159*, 224. <https://doi.org/10.1016/j.jpba.2018.06.055>
- [13] S. W. Tan, N. Gooran, H. M. Lim, B. K. Yoon, J. A. Jackman, *Nanomaterials* **2023**, *13*, 874. <https://doi.org/10.3390/nano13050874>
- [14] J.-B. Farcet, M. Karbiener, L. Zelger, J. Kindermann, T. R. Kreil, *Int. J. Mol. Sci.* **2023**, *24*, 7920. <https://doi.org/10.3390/ijms24097920>
- [15] R. J. Williams, J. N. Phillips, K. J. Mysels, *Trans. Faraday Soc.* **1955**, *51*, 728. <https://doi.org/10.1039/TF9555100728>
- [16] J. N. Phillips, *Trans. Faraday Soc.* **1955**, *51*, 561. <https://doi.org/10.1039/TF9555100561>
- [17] D. Varade, T. Joshi, V. K. Aswal, P. S. Goyal, P. A. Hassan, P. Bahadur, *Colloids Surf., A* **2005**, *259*, 95. <https://doi.org/10.1016/j.colsurfa.2005.02.018>
- [18] M. S. Bakshi, S. Mahajan, *J. Jpn. Oil Chem. Soc.* **2000**, *49*, 17. <https://doi.org/10.5650/jos1996.49.17>
- [19] D. Khatua, A. Gupta, J. Dey, *J. Colloid Interface Sci.* **2006**, *298*, 451. <https://doi.org/10.1016/j.jcis.2005.12.029>
- [20] B. Kopecká, T. Fazekáš, P. Klačík, F. Kopecký, *Tenside, Surfactants, Deterg.* **2009**, *46*, 169. <https://doi.org/10.3139/113.110021>
- [21] M. R. Porter, *Handbook of Surfactants*, Springer, New York, NY **1991**. <https://doi.org/10.1007/978-1-4757-1293-3>
- [22] A. Klimonda, I. Kowalska, *E3S Web Conf.* **2018**, *44*, 00068. <https://doi.org/10.1051/e3sconf/20184400068>
- [23] M. Pérez-Rodríguez, G. Prieto, C. Rega, L. M. Varela, F. Sarmiento, V. Mosquera, *Langmuir* **1998**, *14*, 4422. <https://doi.org/10.1021/la980296a>
- [24] A. Daina, O. Michielin, V. Zoete, *Sci. Rep.* **2017**, *7*, 42717. <https://doi.org/10.1038/srep42717>
- [25] A. Pedretti, A. Mazzolari, S. Gervasoni, L. Fumagalli, G. Vistoli, *Bioinformatics* **2021**, *37*, 1174. <https://doi.org/10.1093/bioinformatics/btaa774>
- [26] C. Zhang, F. Cui, G. Zeng, M. Jiang, Z. Yang, Z. Yu, M. Zhu, L. Shen, *Sci. Total Environ.* **2015**, *518–519*, 352. <https://doi.org/10.1016/j.scitotenv.2015.03.007>
- [27] S. Buffet-Bataillon, P. Tattevin, M. Bonnaure-Mallet, A. Jolivet-Gougeon, *Int. J. Antimicrob. Agents* **2012**, *39*, 381. <https://doi.org/10.1016/j.ijantimicag.2012.01.011>
- [28] S. Wessels, H. Ingmer, *Regul. Toxicol. Pharmacol.* **2013**, *67*, 456. <https://doi.org/10.1016/j.yrtph.2013.09.006>
- [29] M. K. Ijaz, S. A. Sattar, J. R. Rubino, R. W. Nims, C. P. Gerba, *PeerJ* **2020**, *8*, e9914. <https://doi.org/10.7717/peerj.9914>
- [30] B. H. Ogilvie, A. Solis-Leal, J. B. Lopez, B. D. Poole, R. A. Robison, B. K. Berges, *J. Hosp. Infect.* **2021**, *108*, 142. <https://doi.org/10.1016/j.jhin.2020.11.023>
- [31] A. Artasensi, A. Pedretti, G. Vistoli, L. Fumagalli, *Org. Prep. Proced. Int.* **2021**, *53*, 493. <https://doi.org/10.1080/00304948.2021.1956849>
- [32] K. A. Reynolds, *Public Health Microbiology*, Humana Press, Clifton, NJ **2004**. <https://doi.org/10.1385/1-59259-766-1-069>
- [33] A. Wood, D. Payne, *J. Hosp. Infect.* **1998**, *38*(4), 283.
- [34] N. Scholz, T. Behnke, U. Resch-Genger, *J. Fluoresc.* **2018**, *28*, 465. <https://doi.org/10.1007/s10895-018-2209-4>

SUPPORTING INFORMATION

Additional supporting information can be found online in the Supporting Information section at the end of this article.

How to cite this article: S. Strizzi, G. Cappelletti, M. Biasin, A. Artasensi, L. Fumagalli, A. Casiraghi, *Arch. Pharm.* **2023**, e2300424. <https://doi.org/10.1002/ardp.202300424>